Geosci. Model Dev. Discuss., 7, 5341–5380, 2014
www.geosci-model-dev-discuss.net/7/5341/2014/
doi:10.5194/gmdd-7-5341-2014

Geoscientific Model Development Discussions
Open Access

Multi-site evaluation of the JULES land surface model using global and local data

D. Slevin, S. F. B. Tett, and M. Williams

School of Geosciences, The University of Edinburgh, The King's Buildings, West Mains Road, Edinburgh, EH9 3JW, UK

Received: 8 July 2014 – Accepted: 18 July 2014 – Published: 8 August 2014

Correspondence to: D. Slevin (d.slevin@ed.ac.uk)

Published by Copernicus Publications on behalf of the European Geosciences Union.

Abstract

Changes in atmospheric carbon dioxide and water vapour change the energy balance of the atmosphere and thus climate. One important influence on these greenhouse gases is the land surface. Land Surface Models (LSMs) represent the interaction between the atmosphere and terrestrial biosphere in Global Climate Models (GCMs). As LSMs become more advanced, there is a need to test their accuracy. Uncertainty from LSMs contributes towards uncertainty in carbon cycle simulations and thus uncertainty in future climate change. In this study, we evaluate the ability of the JULES LSM to simulate photosynthesis using local and global datasets at 12 FLUXNET sites. Model parameters include site-specific (local) values for each flux tower site and the default parameters used in the Hadley Centre Global Environmental Model (HadGEM) climate model. Firstly, we compare Gross Primary Productivity (GPP) estimates from driving JULES with data derived from local site measurements with driving JULES with data derived from global parameter and atmospheric reanalysis (on scales of 100 km or so). We find that when using local data, a negative bias is introduced into model simulations with yearly GPP underestimated by 16 % on average compared to observations while when using global data, model performance decreases further with yearly GPP underestimated by 30 % on average. Secondly, we drive the model using global meteorological data and local parameters and find that global data can be used in place of FLUXNET data with only a 7 % reduction in total annual simulated GPP. Thirdly, we compare the global meteorological datasets, WFDEI and PRINCETON, to local data and find that the WATCH dataset more closely matches the local meteorological measurements (FLUXNET). Finally, we compare the results from forcing JULES with the remote sensing product MODIS Leaf Area Index (LAI). JULES was modified to accept MODIS LAI at daily timesteps. We show that forcing the model with daily satellite LAI results in only small improvements in predicted GPP at a small number of sites compared to using the default phenology model.

1 Introduction

The atmosphere and biosphere are closely coupled and carbon is transported between the two via the carbon cycle (Cao and Woodward, 1998) and though the carbon cycle is significantly affected by global warming, much still remains to be understood about its behaviour (Schimel, 2007). Of the carbon dioxide emitted into the atmosphere from the burning of fossil fuels, roughly half remains in the atmosphere and the rest is absorbed by carbon sinks on land and in the oceans (Le Quéré et al., 2009). Global warming can affect terrestrial ecosystems in two ways. Firstly, CO_2 fertilisation leads to more uptake of CO_2 by plants, and secondly, a warmer climate can accelerate the decomposition of litter and soil organic carbon, and increase plant respiration. Predictions of the future uptake of atmospheric CO_2 by the terrestrial biosphere are uncertain and this uncertainty comes from whether the terrestrial biosphere will continue to be a sink or source for CO_2. The Coupled Climate–Carbon Cycle Model Intercomparison Project (C4MIP) was the first major study to examine the coupling between climate change and the carbon cycle (Friedlingstein et al., 2006) and one of its main conclusions was the reduced efficiency of the earth system, in particular the land carbon sink, to absorb increased anthropogenic CO_2, but the magnitude of this effect depended on the model used.

Land surface models (LSMs) are an important component of climate models and simulate the interaction between the atmosphere and terrestrial biosphere. They represent the surface energy and water balance, climate effect of snow and carbon fluxes (Pitman, 2003) and are considered the lower boundary condition for Global Climate Models (GCMs) (Best et al., 2011). GCMs require the carbon, water and energy fluxes between the land surface and atmosphere to be specified. Meteorological data, vegetation and soil characteristics are provided as inputs to LSMs, and using these, LSMs can predict fluxes, such as latent and sensible heat, upward longwave radiation and net ecosystem exchange of CO_2, which is used to determine global atmospheric CO_2 concentrations. Various LSMs have been designed over the last 40 years to calculate these fluxes (Dai et al., 2003). They range from the simple "bucket" model of Carson

GMDD
7, 5341–5380, 2014

(1982), which did not take vegetation or soil types into account, to the second generation of land surface models, which attempted to explicitly represent the effects of vegetation in surface energy balance calculations to the current models, in which biochemical models of leaf photosynthesis were developed and linked to the biophysics of stomatal conductance (Farquhar et al., 1980; Bonan, 2008) and can also respond to changes in atmospheric CO_2 in a more realistic way. These LSMs can now describe a comprehensive range of land–atmosphere interactions and be used to understand the response of the biosphere to climate change (Sellers et al., 1997).

LSM components are designed using results from research literature, idealized laboratory experiments and observations from limited field campaigns (Stöckli et al., 2008; Williams et al., 2009). This can lead to sources of uncertainty in the parameterisation of processes and as LSMs become more advanced, there is a need to understand their complexity and accuracy. LSMs can be tested in a variety of ways. Multimodel intercomparison projects provide a measure of how various LSMs behave under controlled conditions (Schaefer et al., 2012; Cadule et al., 2010; Randerson et al., 2009; Dirmeyer et al., 2006; Henderson-Sellers et al., 1996). Parameter perturbation experiments evaluate a single model and numerous simulations are performed where either one parameter is changed at a time within a given range (Knorr, 2000; Knorr and Heimann, 2001; El Maayar et al., 2002) or maximum and minimum values of parameters are used (Hallgren and Pitman, 2000). Recently, in the LSM community, there has been effort to create a more standardised form of model evaluation known as benchmarking, whereby publicly available datasets, at various temporal and spatial resolutions, along with metrics and areas of model performance to be evaluated, are used by different modelling groups to test model performance (Abramowitz, 2012; Luo et al., 2012). This has previously been carried out by Abramowitz et al. (2008) and Blyth et al. (2011).

We identified a gap in the research literature regarding model–observation differences in carbon fluxes when using global and local (site-specific) data by the JULES LSM. Blyth et al. (2011) evaluated JULES at 10 FLUXNET sites, representing a range of biomes and climatic conditions, where model parameter values were taken as if the model was embedded in a GCM, in order to assess the model's ability to predict observed water and carbon fluxes. We extend this work by performing model simulations whereby model parameters are set to local site conditions and compare to those using global and satellite data.

In this study, we use 12 FLUXNET sites that cover a range of ecosystem types; temperate (6), boreal (2), mediterranean (2) and tropical (2) (Table 1), to investigate differences between using local, global and satellite-derived datasets when performing model simulations with JULES version 3.0 (Clark et al., 2011; Best et al., 2011). In particular, we address the following research questions:

- How well does JULES perform when using the best available local meteorological *and* parameter datasets compared to using global data?
- How much error is introduced into site-specific model simulations when using global meteorological data instead of local?
- Of the global meteorological datasets used in this study which one compares best to FLUXNET data?
- Are improvements in simulated GPP observed when forcing JULES with daily satellite phenology compared to using the default phenology module?

2 Methods and model

2.1 Model description

The Joint UK Land Environment Simulator (JULES) is the land surface scheme of the Hadley Centre Global Environmental Model (HadGEM) climate model and evolved from the Met Office Surface Exchange Scheme (MOSES) (Cox et al., 1999). JULES is a mechanistic model and is able to model such processes as photosynthesis, evapotranspiration, soil and snow physics, and soil microbial activity (Blyth et al., 2011). Each

GMDD
7, 5341–5380, 2014

model gridbox is composed of homogeneous surface tiles each representing a particular land cover type (Houldcroft et al., 2009), five of which are vegetation, referred to as Plant Functional Types (PFTs), and four non-vegetation land cover types (Clark et al., 2011).

The surface fluxes of CO_2 associated with photosynthesis are computed on each timestep for each PFT using a coupled photosynthesis-stomatal conductance model (Cox et al., 1998). These accumulated carbon fluxes are passed to TRIFFID (Top-down Representation of Interactive Foliage and Flora Including Dynamics), JULES' dynamic global vegetation model and also its terrestrial carbon cycle component(Cox, 2001) TRIFFID updates the areal coverage, LAI and canopy height for each PFT on a longer timestep (usually every 10 days), based on the net carbon available to it and competition with other vegetation types (Cox, 2001). In JULES, phenology is, typically, updated once per day using accumulated temperature-dependent leaf turnover rates (Clark et al., 2011). GPP is calculated first at leaf-level and then scaled up to canopy-level using LAI for each of the 10 canopy layers. Two versions of JULES were used in this study. JULES3.0 is the original and publicly available release code of JULES version 3.0. The source code can be downloaded from https://jules.jchmr.org/. In addition, JULES3.0 was modified in order to force it with daily MODIS LAI (JULESmod). A more detailed description of JULES can be found in Clark et al. (2011) and Best et al. (2011).

2.2 Experimental design

Offline single point simulations of GPP were performed at each of the 12 flux tower sites using various global and site-specific datasets (Table 2). Correct simulation of GPP is important since errors in its calculation can propagate through the model and affect biomass and other flux calculations (Schaefer et al., 2012). Site-specific (i.e. local) data refers to model parameters and meteorological data that are only relevant for a particular site and global data refers to model parameters taken from datasets used by the global operational version of JULES and meteorological data extracted from global gridded datasets. These study sites were chosen to validate model performance in carbon flux simulation since gap-filled meteorological data, local observations of vegetation and soil characteristics and observed GPP fluxes were available. One year model simulations were performed and span a range of years due to limited availability of local gapfilled meteorological data, observations of GPP fluxes and vegetation characteristics (Table 1). Prior to performing the model simulations, the soil carbon pools at each site were brought to equilibrium using a 10 year spin-up by cycling 5 year averaged meteorological data (in equilibrium mode), followed by a 1000 year spin-up by cycling observed meteorological data (in dynamical mode). At Tumbarumba, Santarem Km67 and Santarem Km83, 3 year averaged meteorological data was used in the first part of the spin-up process due to limited data availability. More information on model spin-up can be found in Clark et al. (2011).

2.2.1 Global vs. local data

Using JULES3.0, we compare model simulations using site-specific parameter and meteorological datasets to those using the default values from the HadGEM model (local-F, global-WEIG, global-WEIC and global-P in Table 2). For these model simulations, the default phenology model (used to update LAI) and TRIFFID were used, but vegetation competition was switched off.

2.2.2 Using global meteorological data instead of local

Using JULES3.0, we quantify how much error is introduced into model simulations when using global (WFDEI-GPCC) instead of local meteorological data (local-WEIG and local-F in Table 2). In these model simulations, the default phenology model is used and vegetation competition has been switched off.

GMDD
7, 5341–5380, 2014

2.2.3 Comparison of global to local meteorological data

The WFDEI-GPCC, WFDEI-CRU and PRINCETON datasets are compared to FLUXNET to find out which one more closely captures the local meteorological conditions.

2.2.4 Daily satellite phenology

Using JULES3.0 and JULESmod, we compare model simulations where JULES is forced with daily MODIS LAI to those where JULES uses the default phenology model (local-FM and local-FNM in Table 2). The phenology and TRIFFID modules have been switched off for the MODIS forced model simulations. Vegetation competition has been switched off for both sets of model simulations. In both cases, the annual maximum LAI is taken to be the annual maximum MODIS LAI and site-specific parameters are used at each flux tower site.

2.3 Data

JULES requires meteorological data at 6 hourly intervals or less in order to drive the model offline. In this study, half-hourly/hourly data was used for model runs using local data and 3 hourly data for simulations using global data. For offline simulations, the model requires downward shortwave and longwave radiation ($\mathrm{W\,m^{-2}}$), rainfall and snowfall rate ($\mathrm{kg\,m^{-2}\,s^{-1}}$), air temperature (K), wind speed ($\mathrm{m\,s^{-1}}$), surface pressure (Pa) and specific humidity ($\mathrm{kg\,kg^{-1}}$). Gap-filled meteorological forcing data at the local scale was obtained from the FLUXNET network and data at the global scale was obtained from two gridded datasets; WATCH (derived from ERA-Interim Reanalysis data) (WFDEI; Weedon et al., 2012, 2011) and that developed by Sheffield et al. (2006) (referred to as PRINCETON).

Vegetation parameters, such as PFT fractions, annual maximum LAI, canopy height, rooting depth and V_{cmax} (maximum rate of Rubisco carboxylase activity), and soil

GMDD
7, 5341–5380, 2014
Multi-site evaluation of the JULES land surface model using global and local data
D. Slevin et al.

texture fractions were adjusted to local or global values depending on the model simulations (Table 2) performed at the 12 flux tower sites. Site-specific vegetation and soil parameters were obtained from the research literature, communications with site Primary Investigator and the Ameriflux data archive. Global vegetation and soil parameters were derived from datasets used in the global operational version of the model. The satellite LAI data used to force JULES was obtained from the MODerate resolution Imaging Spectroradiometer (MODIS) instrument aboard NASA's Earth Observing System (EOS) satellites, Terra and Aqua (http://modis.gsfc.nasa.gov).

2.3.1 Forcing data

FLUXNET, a "network of regional networks", is a global network of micrometeorological tower sites that measure the exchange of carbon dioxide, water vapour and energy between the biosphere and atmosphere across a range of biomes and timescales (Baldocchi et al., 2001). Data and site information are available at http://www.fluxnet.ornl.gov/. Over 500 tower sites are located worldwide on five continents and are used to study a range of vegetation types such as temperate conifer and broadleaved (deciduous and evergreen) forests, tropical and boreal forests, crops, grasslands, wetlands, and tundra (Baldocchi et al., 2001).

The WATCH Forcing Data (WFD) was created in the framework of the Water and Global Change (WATCH) project (http://www.eu-watch.org/), which sought to assess the terrestrial water cycle using land surface models and general hydrological models, and was derived using the 40 yr ECMWF Re-Analysis (ERA-40) for 1958–2001 and reordered reanalysis data for 1901–1957(Weedon et al., 2011). WFD was extended by applying the WFD methodology to the ERA-Interim data (WFDEI) for the 1979–2009 period (Weedon et al., 2012). Within WFD and WFDEI, there are two precipitation products, the first corrected using the Climate Research Unit at the University of East Anglia (CRU) observations and the second using Global Precipitation Climatology Centre (GPCC) observations. The WFDEI datasets incorporating the GPCC- and CRU-corrected precipitation products are referred to as WFDEI-GPCC and WFDEI-CRU,

GMDD
7, 5341–5380, 2014

respectively. WFDEI is only available for land points including Antarctica, and consists of 3 hourly, regularly (latitude-longitude) gridded data at half-degree ($0.5^\circ \times 0.5^\circ$) resolution. The Sheffield et al. (2006) dataset (PRINCETON) is a global 50 yr meteorological dataset for driving land surface models developed by the Land Surface Hydrology Research Group at Princeton University. It consists of 3 hourly, 1° resolution, meteorological data for the 1948–2008 period.

2.3.2 Ecological and soil data

The Global Land Cover Characterization (version 2) database (http://edc2.usgs.gov/glcc/glcc.php), generated by the US Geological Survey, the University of Nebraska-Lincoln, and the European Commission's Joint Research Centre, is a 1 km resolution global land cover dataset for use in environmental and modelling research (Loveland et al., 2000). Land cover is classified into 17 categories using the International Geosphere–Biosphere Programme (IGBP) scheme. Each flux tower site is defined by one of these categories and the corresponding vegetation characteristics, such as land cover fractions, LAI and canopy height of PFTs, are derived from look-up tables used in the global operational version of the model.

Global soil texture fractions (% of sand, silt and clay) for each of the 12 FLUXNET sites (not shown here) were extracted from the Harmonized World Soil Database (version 1.2) (HWSD) (Nachtergaele et al., 2012). The equations used to compute soil hydraulic and thermal characteristics were taken from the Unified Model Documentation Paper No 70 (Jones, 2007). Note that the equations in Jones (2007) apply only to mineral soils, as organic soils behave differently (Gornall et al., 2007). In this study, the soils are classified as mineral at all 12 sites. Since the HWSD contains soil textures for two soil depths (0–30 and 30–100 cm) and JULES contains four soil layers (thicknesses of 0.1, 0.25, 0.65 and 2.0), the 0–30 cm soil textures were assigned to the top two model soil layers (thicknesses 0.1 and 0.25 m, respectively), and the 30–100 cm textures were assigned to the bottom two layers (thicknesses 0.65 and 2.0 m,

GMDD
7, 5341–5380, 2014

respectively). The site-specific soil textures are provided as site averages and therefore, each model soil layer (4 in total) is assigned the same set of soil textures.

2.3.3 MODIS LAI products

The MODIS LAI product, computed from MODIS spectral reflectances, provides continuous and consistent LAI coverage for the entire global land surface at 1 km resolution (Yang et al., 2006). Some gaps and noise in the data are possible due to the presence of cloudiness, seasonal snow cover and instrument problems, and this can limit the usefulness of the product (Gao et al., 2008; Lawrence and Chase, 2007). In this study, we use the MODIS Land Product Subsets, created by the Oak Ridge National Laboratory Distributed Active Archive Center (ORNL DAAC), which provide summaries of selected MODIS Land Products for use in model validation and field site characterisation and include data for more than 1000 field sites and flux towers (http://daac.ornl.gov/MODIS/).

The MODIS Land Product Subsets (ASCII format) contain LAI data for a 7 km × 7 km grid of 49 pixels, with each pixel representing the 1 km × 1 km scale, at 8 day composite intervals. The average of the 3 × 3 gridbox (pixels 17, 18, 19, 24, 25, 26, 31, 32 and 33) centred on the flux tower, pixel 25, is taken to be that day's LAI value. Only pixel values with an even quality control (QC) flag was used for the averaging and this produced a time-series of 8 day observations at each of the sites. Missing data were dealt with by using the previous good value in the time-series. The exception to this was Bondville, where missing data occurred in January 2000 (this year was used due to limited data availability at Bondville), since MODIS only started recording data in February 2000. To gap-fill the missing data, an 11 year average was computed and the missing data replaced with the average for January 2000. Finally, each time-series of 8 day composite values was linearly interpolated to obtain a daily LAI time-series.

GMDD
7, 5341–5380, 2014

2.4 Model analyses

To quantify differences between output from the various model simulations and observations, we used Root Mean Squared Error (RMSE) (Eq. 1), which is a measure of the average error of the simulations, and bias (Eq. 2), which is the average difference between model and observations (a measure of under- or overprediction).

$$\mathrm{RMSE} = \sqrt{\frac{\sum_{t=1}^{t=n}(x_t - x_{\mathrm{o},t})^2}{n}} \tag{1}$$

$$\mathrm{Bias} = \frac{\sum_{t=1}^{t=n} x_t - \sum_{t=1}^{t=n} x_{\mathrm{o},t}}{n} \tag{2}$$

x_t and $x_{\mathrm{o},t}$ are model and observed daily GPP fluxes, respectively, which have been smoothed using a 7 day moving average since we are interested in the long-term average and not daily variability. n is the number of paired values (number of days in year).

3 Results

3.1 Global vs. local fluxes

When driven with local meteorological and parameter datasets (local-F; Fig. 1), JULES has a negative bias with yearly GPP underestimated by 16 % (3069 g C m^{-2} year^{-1}) on average across all sites compared to observations. By using local data, JULES performs very well at the temperate forest sites, Harvard Forest, Morgan Monroe, Hyytiala and Tharandt, where RMSEs range from 1.1–1.4 g C m^{-2} day^{-1} and biases from −0.2 to +0.3 g C m^{-2} day^{-1}, but performs very poorly at Tumbarumba, El Saler, Bondville and Vaira Ranch and the tropical sites, Santarem Km67 and Santarem Km83, with RMSEs ranging from 1.8–4.1 g C m^{-2} day^{-1} and biases from −3.7 to −0.2 g C m^{-2} day^{-1} (Fig. 2a).

GMDD
7, 5341–5380, 2014

At the temperate forest sites, JULES simulates the summer carbon uptake and leaf onset and senescence quite well. For example, at the needleleaf forests, Hyytiala and Tharandt, the model correctly captures the timing and magnitude of the seasonal cycle of GPP (Fig. 1). JULES is able to capture the beginning and ending of the growing season, but underestimates the summer carbon uptake at the temperate sclerophyll forest, Tumbarumba (Fig. 1). At the tropical sites, the seasonal cycle has been modelled very poorly with annual GPP being underestimated by 42 % (1340 $\mathrm{g\,C\,m^{-2}\,year^{-1}}$) and 21 % (583 $\mathrm{g\,C\,m^{-2}\,year^{-1}}$), respectively.

By replacing the local data with global meteorological and parameter values, JULES had a much greater negative bias with yearly GPP underestimated by 30 % (6706 $\mathrm{g\,C\,m^{-2}\,year^{-1}}$) on average across all sites compared to observations (global-WEIG, global-WEIC and global-P; Fig. 1). This is also shown in the annual average GPP which has been plotted for each of the model simulations and observations at the 12 sites (Fig. 1). This trend occurs at all sites, with the exception of the wetland site, Kaamanen, and Santarem Km83, where modelled yearly GPP (2684 $\mathrm{g\,C\,m^{-2}\,year^{-1}}$ and 492 $\mathrm{g\,C\,m^{-2}\,year^{-1}}$, respectively) is overestimated (global-P; Table 2) compared to model runs using only local data (2141 $\mathrm{g\,C\,m^{-2}\,year^{-1}}$ and 119 $\mathrm{g\,C\,m^{-2}\,year^{-1}}$, respectively).

We found the meteorological data had a greater impact on modelled GPP fluxes than model parameters. Larger differences exist between local-WEIG and local-F ($\mathrm{local_{WEIG-F}}$; Fig. 2d), which differ only in the atmospheric forcings dataset used, compared to between global-WEIG and local-WEIG (global – $\mathrm{local_{WEIG}}$; Fig. 2e), which differ only in the model parameter sets used.

The ability of JULES to capture yearly GPP (bias) and the seasonal cycle (RMSE) is affected at the majority of sites when using global meteorological data (Fig. 2d), with significant changes observed at Santarem Km67 and Santarem Km83. However, model parameters were found to affect bias at all 12 sites (Fig. 2e) with the tropical sites being the most influenced. With the exception of Tumbarumba, biases associated with meteorological data compensate for those associated with model parameters at the tropical sites ($\text{global}_{\text{WEIG}} - \text{local}_{\text{F}}$; Fig. 2c).

Overall, JULES performs very well with the use of local data (meteorological and parameter datasets) with negative biases observed at the tropical sites and the Southern Hemisphere site, Tumbarumba. Improvements included the beginning and ending of the growing season. We found the opposite to be the case with the use of global data, with JULES performing worse at most sites, with the exception of the tropical sites. We found the meteorological data to have a greater effect on GPP fluxes than the model parameters.

3.2 Global meteorological data

As well as quantifying differences in model simulations using either local or global data, it is useful to know how global meteorological data affects site-specific model runs. Global meteorological data can be used in place of FLUXNET data in order to drive JULES (local-WEIG; Table 2). This is important for ecological research sites where there is limited or no local meteorological data available. Using the WFDEI-GPCC dataset to force the model increases the negative bias of model simulations using local parameters (local-WEIG; Fig. 2f) with a 7 % reduction in total annual simulated GPP (15 469 $\text{g C m}^{-2}\,\text{year}^{-1}$ for local-F reduced to 14 193 $\text{g C m}^{-2}\,\text{year}^{-1}$ for local-WEIG).

Forcing the model with WFDEI-GPCC (local-WEIG) results in decreases in model performance (increases in bias and RMSE) at the majority of sites. The tropical sites, Santarem Km67 and Santarem Km83, are two exceptions and show a noticeable improvement in modelled yearly GPP (66 % and 61 % reduction of bias, respectively) and changes to modelled seasonal cycle (25 % increase and 65 % reduction of RMSE, respectively). However, forcing the model with global meteorological data introduces very small errors into GPP predictions at Tharandt, Kaamanen and Hyytiala, where RMSEs range from 1.1–1.3 $\text{g C m}^{-2}\,\text{year}^{-1}$ (Fig. 2f).

Discussion Paper | Discussion Paper | Discussion Paper | Discussion Paper |

GMDD

7, 5341–5380, 2014

Multi-site evaluation of the JULES land surface model using global and local data

D. Slevin et al.

Overall, driving JULES with global meteorological data introduces biases into single site simulations. At the majority of sites, these biases are negative, but at tropical sites, the global meteorological data improves model performance.

3.3 Global vs. local meteorological data

As well as quantifying the error introduced into model simulations by using global atmospheric forcing data instead of local, we also compare the global meteorological data to local. Only the downward shortwave and longwave radiation fluxes, precipitation and surface air temperature variables have been compared to FLUXNET values, since these variables play the most influential role of the meteorological forcings in canopy photosynthesis and light propagation in JULES (Alton et al., 2007). In order to compare the atmospheric forcing data, it was first converted to dimensionless quantities by dividing the daily time series by the annual mean before computing the bias and RMSE.

Of the two global meteorological datasets used in this study, the WFDEI dataset compares best to FLUXNET at the majority of sites (Fig. 3). Surface air temperatures compare best to local meteorological measurements with average RMSEs of 0.4 % and 0.7 % (7 day filtered RMSE expressed as percentages of the annual mean value) (1.5 K and 2.4 K) across all sites for the WFDEI and PRINCETON datasets, respectively (Fig. 3d), followed by the downward shortwave radiation fluxes with average RMSEs of 13 % and 17 % (27.0 $\mathrm{W\,m^{-2}}$ and 33.2 $\mathrm{W\,m^{-2}}$) for WFDEI and PRINCETON, respectively (Fig. 3a), and downward longwave radiation fluxes with average RMSEs of 4 % and 5 % (18.9 $\mathrm{W\,m^{-2}}$ and 25.0 $\mathrm{W\,m^{-2}}$) for WFDEI and PRINCETON, respectively (Fig. 3b). Precipitation data from global datasets differ most from local values with RMSEs of 112–178 % (2.7–4.4 $\mathrm{mm\,day^{-1}}$) for WFDEI-GPCC, WFDEI-CRU and PRINCETON, respectively, which may be due to how the precipitation products of each global dataset is corrected(Weedon et al., 2011; Sheffield et al., 2006).

In addition to comparing the global meteorological variables to their local values, we also examine the two precipitation products, WFDEI-GPCC (GPCC-corrected) and

GMDD
7, 5341–5380, 2014

WFDEI-CRU (CRU-corrected), within the WFDEI dataset. We found WFDEI-GPCC and WFDEI-CRU compare equally well at the 12 FLUXNET sites (Fig. 3c) with average of RMSEs of 2.7 and 2.8 mm day^{-1}, respectively. Differences between GPCC- and CRU-corrected precipitation RMSEs are small (0.0–1.4 g C m^{-2} day^{-1}) at individual flux tower sites. When forcing JULES with WFDEI, there is little difference when either WFDEI-GPCC or WFDEI-CRU is used as the precipitation product, with average RMSEs of 2.9 and 2.8 g C m^{-2} day^{-1}, respectively, across all sites, although differences in the datasets may be more important when JULES is run globally.

Even though WFDEI compares better to the local meteorological data than PRINCETON, we found that when JULES is forced with the PRINCETON dataset, significant improvements in GPP predictions were observed at Santarem Km67 and Santarem Km83 (Fig. 1). We observed that at the tropical sites, the meteorological forcings were the primary driver of productivity for model simulations using global data and that biases associated with the global meteorological data compensated for incorrect parameter values (Sect. 3.1). By swapping the local meteorological data with global data, the positive bias associated with global surface air temperature (PRINCETON) at Santarem Km83 is the primary cause of improved model performance (39 % reduction in RMSE) and by forcing JULES with the PRINCETON dataset and using the lower global V_{cmax} value (Table 4), the model was able to reproduce the seasonal cycle very well (RMSE of 1.26 g C m^{-2} day^{-1}). At Santarem Km67, we found the downward longwave radiation to be the main reason for the improved seasonal cycle (35 % reduction in RMSE) and by using the PRINCETON dataset and global V_{cmax} value (Table 4), model performance was significantly improved (RMSE of 2.12 g C m^{-2} day^{-1}).

Compensation between meteorological data and model parameters also occurs at Hyytiala, where the model performs very well with global meteorological and parameter datasets (Fig. 1). The global downward shortwave radiation is larger than its locally measured value and this offsets the low global V_{cmax} value at this site (Table 4, Fig. 5b).

Overall, we found the WFDEI dataset compares better than PRINCETON to FLUXNET and of the four meteorological variables examined, the radiation fluxes

GMDD
7, 5341–5380, 2014

(downward shortwave and longwave) and surface air temperatures compare quite well to local values. Within the WFDEI dataset, the two precipitation products (WFDEI-GPCC and WFDEI-CRU) compare equally well to FLUXNET precipitation. Significant improvements were observed at the tropical sites when JULES is forced with PRINCETON, but this is due to biases associated with the meteorological data.

3.4 Forcing JULES with daily satellite phenology

The performance of LSMs depend on how well the seasonal variation of LAI is represented since GPP is strongly influenced by the timing of budburst and leaf senescence (Liu et al., 2008). In JULES, LAI is essential for the calculation of plant canopy photosynthesis and is updated daily in response to temperature. We test the JULES phenology model by comparing model predictions of GPP when JULES uses its default phenology model with those in which JULES uses local data with the annual maximum LAI set to be the MODIS annual maximum LAI (local-FNM) and with those in which the model uses local data and is forced with daily MODIS LAI (local-FM).

Forcing JULES with daily satellite LAI (local-FM) results in either small improvements in predicted GPP or none at all at the 12 flux tower sites (Fig. 4c). An average RMSE of 2.2 $\mathrm{g\,C\,m^{-2}\,day^{-1}}$ across all sites is observed when the model is forced with daily MODIS LAI (local-FM). This is a small improvement in model performance compared to using no MODIS information (local-F; average RMSE of 2.4 $\mathrm{g\,C\,m^{-2}\,day^{-1}}$) and setting the annual maximum MODIS LAI to be the annual maximum LAI at each site (local-FNM; average RMSE of 2.39 $\mathrm{g\,C\,m^{-2}\,day^{-1}}$).

By using MODIS data, there is only a small reduction in average RMSE (8 % and 0.04 % for local-FM and local-FNM, respectively) when simulating GPP compared to model runs which do not use it. Of the 12 sites, only seven (Harvard Forest, Vaira Ranch, Hyytiala, Tharandt, Tumbarumba, Kaamanen and Santarem Km67) show improved model performance when either being forced with daily MODIS LAI (Fig. 4c) or using the annual maximum MODIS LAI as the model annual maximum LAI (Fig. 4b). At

GMDD
7, 5341–5380, 2014

these 7 sites, simulated yearly GPP increases in total by 21 %. At the remaining sites, JULES performs better using the default phenology module (Fig. 4a).

Of the seven sites, where JULES' performance improved using MODIS data, forcing JULES with daily satellite phenology (local-FM) only resulted in improved model performance at Santarem Km67 (Fig. 4c) and at the remaining six sites, using the default phenology with the annual maximum MODIS LAI set to be the annual maximum LAI (Fig. 4b), JULES' performance improved. Even with the addition of MODIS data, the model still performed poorly at Bondville, with only a slight improvement in predicted GPP (RMSEs of 3.62 $\mathrm{g\,C\,m^{-2}\,day^{-1}}$) and 3.15 $\mathrm{g\,C\,m^{-2}\,day^{-1}}$) for local-FM and local-FNM, respectively) compared to using only local data (RMSE of 3.66 $\mathrm{g\,C\,m^{-2}\,day^{-1}}$).

The sites which display the largest improvements in simulated GPP, when forced with MODIS LAI, are those which have low LAI values (54 % and 24 % reduction in RMSE at Vaira Ranch and Fort Peck, respectively) (Fig. 4c). Small improvements were also observed at the tropical sites (13 % and 14 % reduction in RMSE at Santarem Km67 and Santarem Km83, respectively). At some sites, using MODIS data had no effect on model results (El Saler) and in some cases, the model performed worse (Tumbarumba).

The total annual simulated GPP for model runs using MODIS data (15 334 and 15 227 $\mathrm{g\,C\,m^{-2}\,year^{-1}}$, for local-MF and local-NMF, respectively) is slightly lower than when using only local data (15 469 $\mathrm{g\,C\,m^{-2}\,year^{-1}}$), but better than when using global data (global-WEIG; 14 193 $\mathrm{g\,C\,m^{-2}\,year^{-1}}$). This is a result of the annual maximum MODIS LAI being closer to local values than global (Fig. 4a). The increased LAI of the global data does not result in increased GPP predictions since the meteorological data and vegetation parameters, such as V_{cmax}, may have a greater impact on predicted GPP than LAI.

Overall, when JULES is forced with daily MODIS LAI small improvements in predicted GPP are observed at a number of sites, though there exists a negative bias associated with using MODIS data. By setting the annual maximum MODIS LAI to be the annual maximum LAI at each site, the model performs equally well to site-specific model simulations. We also observed significant improvements in simulated GPP at sites with low LAI values, such as grasslands, when JULES is forced with daily LAI.

4 Discussion

4.1 How well does JULES perform when using the best available local meteorological and parameter datasets compared to using global data?

At more than half of the sites, JULES performs very well when using local meteorological and parameter datasets with a negative bias observed for the remaining sites (Fig. 2). However, the use of global meteorological and parameter datasets introduces a negative bias into GPP simulations at all sites with the exception of the tropical sites.

Our results compare well with the evaluation of JULES by Blyth et al. (2011), where parameters were obtained as though the model was embedded in a GCM. Differences between the two studies include different model versions and global meteorological datasets used. As shown by Blyth et al. (2011), we also found simulated photosynthesis to be underestimated for the temperate forests (Harvard Forest, Tharandt and Morgan Monroe), grasslands (Fort Peck), mediterranean sites (El Saler) and the tropical forests (Santarem Km67), and overestimated for the wetlands (Kaamanen). We observed that the use of local observations of site characteristics, such as PFT fractions and vegetation properties, lead to significant improvements in model performance at more than half of the sites (Fig. 2a), though errors still exist with biases ranging from -1 to $1\,\mathrm{g\,C\,m^{-2}\,day^{-1}}$ and RMSEs from 1 to $2\,\mathrm{g\,C\,m^{-2}\,day^{-1}}$.

Differences between global and local data include PFT fractions (Table 3), soil texture fractions, vegetation parameters (Table 4) and atmospheric forcing data. At some sites, such as Bondville and Santarem Km67/Km83, the global and local values for LAI and V_{cmax} were markedly different (Fig. 5), though for the majority of sites, global and local LAI values are quite close (Fig. 5a), whereas global V_{cmax} values were underestimated compared to local values (below dashed line in Fig. 5b). MODIS LAI values tend to

GMDD
7, 5341–5380, 2014

more closely match the local values and in general, were lower than global values (Fig. 5a).

In general, we found the meteorological data to play a more important role than model parameters in determining GPP fluxes at sites, such as Santarem Km67 and Santarem Km83. At these sites, the meteorological forcing data was the primary driver of productivity and biases associated with the global meteorological data compensated for incorrect parameter values. However, at Tumbarumba, incorrectly predicted GPP was due to model error rather than meteorological data or model parameters. We performed a temperature sensitivity study at Tumbarumba using local meteorological and parameter datasets (local-F) and observed improved simulations of winter carbon release with increasing temperatures.

4.2 How much error is introduced into site-specific model simulations when using global meteorological data instead of local?

Using global meteorological data to drive JULES increases the negative bias of site-specific model simulations (local-WEIG; Fig. 2f). We observed decreases in model performance at the majority of sites, with the exceptions being the tropical sites (Santarem Km67/Km83). At some sites, such as Hyytiala and Kaamanen, using global meteorological data produced similar results to using FLUXNET data.

Therefore, forcing JULES with WFDEI introduces significant errors into single-point model simulations and means that global meteorological data may not be used in place of local data at sites with limited or no meteorological data.

4.3 Of the global meteorological datasets used in this study which one compares best to FLUXNET data?

At the majority of sites, the WFDEI dataset compared best to local meteorological measurements (Fig. 3). This is likely due to the WFDEI dataset being derived from the ECMWF Re-analysis (ERA-Interim) dataset (Dee et al., 2011), which is a higher

GMDD
7, 5341–5380, 2014

resolution dataset and uses a more advanced data assimilation system than the NCEP-NCAR Re-analysis, from which the PRINCETON dataset is derived (Kistler et al., 2001).

At the sites considered, differences between global and local values for downward shortwave and longwave radiation fluxes and surface air temperatures are quite small (Fig. 3a, b and d), while significantly larger differences are observed for precipitation (Fig. 3c). At the majority of sites, there is a negative bias associated with precipitation (Fig. 3c), but this will have little effect on GPP fluxes since JULES is relatively insensitive to precipitation (Galbraith et al., 2010). For the remaining meteorological variables, there is a positive bias associated with surface air temperature, but no dominant bias associated with the radiation fluxes. However, at individual sites, biases associated with the meteorological driving data can affect model results.

4.4 Are improvements in simulated GPP observed when forcing JULES with daily satellite phenology compared to using the default phenology module?

In general, we found that using MODIS data resulted in only small decreases in RMSE at a limited number of sites compared to using locally observed LAI. At sites where model performance improved, improvements were a result of setting the annual maximum LAI to be the annual maximum MODIS LAI rather than forcing the model with daily MODIS LAI. The largest improvements in simulated GPP occur at sites with low annual LAI, such as the grassland (Vaira Ranch, Fort Peck, Kaamanen) and cropland (Bondville) sites and the tropical sites (Santarem Km67 and Santarem Km83). At the boreal sites, Tharandt and Hyytiala, the MODIS LAI tended to be quite noisy and this led to underestimated GPP (Fig. 4c).

We found that at sites where the MODIS LAI timeseries was noisy, this resulted in decreased model performance. At some of the flux tower sites, the MODIS data failed to capture aspects of the seasonal cycle of leaf phenology, such as the magnitude of the seasonal cycle (Tharandt, El Saler) and the beginning and end of the growing season (Bondville). For example, at Tumbarumba, the MODIS instrument estimated the

GMDD
7, 5341–5380, 2014

annual maximum LAI to be 6.08 m^{-2} m^{-2} and the daily LAI to be quite noisy whereas the ground level observations show it to be 2.5 m^{2} m^{-2} (Table 4) and LAI to be constant for much of the year.

The MODIS instrument provides a valuable source of information that can be used by land surface models. However, in this study, the quality of the LAI data can affect model performance. At the tropical sites, MODIS was unable to capture the magnitude of seasonal variation in LAI with MODIS overestimating the locally observed annual maximum LAI at Santarem Km67 and Santarem Km83 by 28 % and 10 %, respectively (Table 4). It was also unable to correctly capture LAI during the Amazonian rainy season, which runs from December to June, as a result of increased cloud cover. The MODIS LAI is very noisy in these regions, but should be constant through out the year.

Overall, we found the model's phenology module performed quite well at the temperate sites with poor performance observed at the tropical and cropland sites. The ability of the phenology model to simulate GPP fluxes reasonably well at temperate sites, with slight underestimation of the summer carbon uptake and phase shift (leaf onset and senescence), may be due to its design (temperate-dependent for the BL PFT class) and the choice of model parameters for BL/NL PFT classes. Forcing the model with MODIS LAI only slightly improved model performance. However, setting the annual maximum LAI for each PFT to be the annual maximum MODIS LAI resulted in improved model performance, without the computational overhead of forcing JULES with daily satellite data. More accurate GPP predictions can be possible with a phenology model modified to take tropical regions into account and associated model parameters for tropical PFTs.

5 Conclusions

We performed a multi-site evaluation of the JULES LSM using site-specific, global and satellite data. In general, we found that when using local meteorological and parameter datasets, JULES performed quite well at temperate sites with a negative bias observed at the tropical and cropland sites. The use of global data worsens model performance by introducing negative biases into model simulations of GPP at the majority of sites with the exception of the tropical sites. The improvement in model simulated GPP when using site-specific values of vegetation properties implies that global values may be incorrect and at sites where model performance improved using global data, this was due to biases associated with the meteorological data. We observed that the meteorological data had a greater impact on modelled GPP fluxes than model parameters.

The use of meteorological data extracted from global atmospheric forcing datasets was used to drive JULES. We found that global meteorological data increased the negative biases of site-specific model simulations at all sites with the exception of the tropical sites, where GPP predictions were improved. Of the two global meteorological datasets used in this study, the WFDEI dataset more closely captures the local meteorological conditions, though we found that the PRINCETON dataset results in improved performance at some of the sites due to positive biases associated with the downward radiation fluxes and surface air temperature.

LAI is an important parameter used in the calculation of canopy photosynthesis. Small improvements in model performance were observed with the use of MODIS data compared to using local meteorological and parameter data. Using MODIS data for the annual maximum LAI allows for improved model performance without the complication of assimilating daily satellite data into the model. We found the default phenology module allowed JULES to perform reasonably well at temperate sites, but not at the tropical sites. More realistic simulation of the seasonal cycle of GPP was observed at sites with low LAI values, such as the grasslands, but this may be, in addition to more accurate LAI data, due to model parameters for the C3 PFT class being more accurate than for the other PFT classes.

Although only a limited number of model parameters were modified at the 12 flux tower sites, due to limited data availability at FLUXNET sites, we showed that with more accurate information regarding flux tower sites, improved predictions of GPP are possible. However, negative biases still exist in this situation and is due to model error

GMDD
7, 5341–5380, 2014

and incorrect modelling of tropical processes. We suggest that improved model performance with regards to the terrestrial carbon cycle can be achieved with the introduction of more PFT classes and their associated model parameters and a phenology model which can properly simulate carbon fluxes in both temperate and tropical regions.

Acknowledgements. This work was carried out during D. Slevin's PhD research and was funded by a School Scholarship from the School of Geosciences, University of Edinburgh. For site-specific parameter data, we would like to thank the following people: Danilo Dragoni (Morgan Monroe), Bill Munger (Harvard Forest), Thomas Grünwald (Tharandt), Pasi Kolari (Hyytiala), Eva Van Gorsel (Tumbarumba) and Ray Leuning (Tumbarumba). Chris Jones and Andy Wiltshire at the UK Met Office kindly provided information on the global parameter data used by the global operational version of JULES. Graham Weedon (UK Met Office) provided advice on using the WATCH (ERA-Interim) dataset. The authors gratefully acknowledge advice from Tristan Quaife (Reading University) and Jose Gómez-Dans (University College London) on using the MODIS data and Doug Clark at the Centre for Ecology and Hydrology (CEH) on model spin-up.

References

Abramowitz, G.: Towards a public, standardized, diagnostic benchmarking system for land surface models, Geosci. Model Dev., 5, 819–827, doi:10.5194/gmd-5-819-2012, 2012. 5344

Abramowitz, G., Leuning, R., Clark, M., and Pitman, A.: Evaluating the performance of land surface models, J. Climate, 21, 5468–5481, 2008. 5344

Alton, P., Mercado, L., and North, P.: A sensitivity analysis of the land-surface scheme JULES conducted for three forest biomes: biophysical parameters, model processes, and meteorological driving data, Global Biogeochem. Cy., 20, GB1008, doi:10.1029/2005GB002653, 2007. 5355

Aurela, M., Tuovinen, J.-P., and Laurila, T.: Carbon dioxide exchange in a subarctic peatland ecosystem in northern Europe measured by the eddy covariance technique, J. Geophys. Res.-Atmos., 103, 11289–11301, 1998. 5375

GMDD

7, 5341–5380, 2014

Multi-site evaluation of the JULES land surface model using global and local data

D. Slevin et al.

Title Page

Abstract | Introduction

Conclusions | References

Tables | Figures

◂ | ▸

Back | Close

Full Screen / Esc

Printer-friendly Version

Interactive Discussion

Baldocchi, D., Falge, E., Gu, L. H., Olson, R., and Hollinger, D.: FLUXNET: a new tool to study the temporal and spatial variability of ecosystem-scale carbon dioxide, water vapor, and energy flux densities, B. Am. Meteorol. Soc., 82, 2415–2434, 2001. 5349

Beerling, D. J. and Quick, W. P.: A new technique for estimating rates of carboxylation and electron transport in leaves of C3 plants for use in dynamic global vegetation models, Glob. Change Biol., 1, 289–294, 1995. 5375

Best, M. J., Pryor, M., Clark, D. B., Rooney, G. G., Essery, R.L. H., Ménard, C. B., Edwards, J. M., Hendry, M. A., Porson, A., Gedney, N., Mercado, L. M., Sitch, S., Blyth, E., Boucher, O., Cox, P. M., Grimmond, C. S. B., and Harding, R. J.: The Joint UK Land Environment Simulator (JULES), model description – Part 1: Energy and water fluxes, Geosci. Model Dev., 4, 677–699, doi:10.5194/gmd-4-677-2011, 2011. 5343, 5345, 5346

Blyth, E., Gash, J., Lloyd, A., Pryor, M., Weedon, G. P., and Shuttleworth, J.: Evaluating the JULES land surface model energy fluxes using FLUXNET data, J. Hydrometeorol., 11, 509–519, 2010. 5375

Blyth, E., Clark, D. B., Ellis, R., Huntingford, C., Los, S., Pryor, M., Best, M., and Sitch, S.: A comprehensive set of benchmark tests for a land surface model of simultaneous fluxes of water and carbon at both the global and seasonal scale, Geosci. Model Dev., 4, 255–269, doi:10.5194/gmd-4-255-2011, 2011. 5344, 5345, 5359

Bonan, G. B.: Forests and climate change: forcings, feedbacks, and the climate benefits of forests, Science, 320, 1444–1449, 2008. 5344

Bruno, R. D., Da Rocha, H. R., De Freitas, H. C., Goulden, M. L., and Miller, S. D.: Soil moisture dynamics in an eastern Amazonian tropical forest, Hydrol. Process., 20, 2477–2489, 2006. 5375

Cadule, P., Friedlingstein, P., Bopp, L., Sitch, S., Jones, C. D., Ciais, P., Piao, S. L., and Peylin, P.: Benchmarking coupled climate–carbon models against long-term atmospheric CO_2 measurements, Global Biogeochem. Cy., 24, GB2016, doi:10.1029/2009GB003556, 2010. 5344

Cao, M. and Woodward, F. I.: Dynamic responses of terrestrial ecosystem carbon cycling to global climate change, Nature, 393, 249–252, 1998. 5343

Carson, D. J.: Current parameterizations of land-surface processes in atmospheric general circulation models, in: Land Surface Processes in Atmospheric General Circulation Models, Cambridge University Press, Cambridge, UK, 67–108, 1982. 5343

Clark, D. B., Mercado, L. M., Sitch, S., Jones, C. D., Gedney, N., Best, M. J., Pryor, M., Rooney, G. G., Essery, R. L. H., Blyth, E., Boucher, O., Harding, R. J., Huntingford, C., and

GMDD
7, 5341–5380, 2014

Multi-site evaluation of the JULES land surface model using global and local data

D. Slevin et al.

Cox, P. M.: The Joint UK Land Environment Simulator (JULES), model description – Part 2: Carbon fluxes and vegetation dynamics, Geosci. Model Dev., 4, 701–722, doi:10.5194/gmd-4-701-2011, 2011. 5345, 5346, 5347

Cleugh, H. A., Leuning, R., Mu, Q., and Running, S. W.: Regional evaporation estimates from flux tower and MODIS satellite data, Remote Sens. Environ., 106, 285–304, 2007. 5375

Cox, P., Huntingford, C., and Harding, R.: A canopy conductance and photosynthesis model for use in a GCM land surface scheme, J. Hydrol., 212, 79–94, 1998. 5346

Cox, P. M.: Description of the TRIFFID Dynamic Global Vegetation Model, Hadley Centre Technical Note, 24, 1–16, 2001. 5346

Cox, P. M., Betts, R. A., Bunton, C. B., Essery, R. L. H., Rowntree, P. R., and Smith, J.: The impact of new land surface physics on the GCM simulation of climate and climate sensitivity, Clim. Dynam., 15, 183–203, 1999. 5345

Dai, Y., Zeng, X., Dickinson, R. E., Baker, I., Bonan, G. B., Bosilovich, M. G., Denning, A. S., Dirmeyer, P. A., Houser, P. R., Niu, G., Oleson, K. W., Schlosser, C. A., Yang, Z.- L.: The Common Land Model, B. Am. Meteorol. Soc., 84, 1013–1023, 2003. 5343

Dee, D. P., Uppala, S. M., Simmons, A. J., Berrisford, P., Poli, P., Kobayashi, S., Andrae, U., Balmaseda, M. A., Balsamo, G., Bauer, P., Bechtold, P., Beljaars, A. C. M., van de Berg, L., Bidlot, J., Bormann, N., Delsol, C., Dragani, R., Fuentes, M., Geer, A. J., Haimberger, L., Healy, S. B., Hersbach, H., Hólm, E. V., Isaksen, L., Kållberg, P., Köhler, M., Matricardi, M., McNally, A. P., Monge-Sanz, B. M., Morcrette, J.-J., Park, B.-K., Peubey, C., de Rosnay, P., Tavolato, C., Thépaut, J.-N., and Vitart, F.: The ERA-Interim reanalysis: configuration and performance of the data assimilation system, Q. J. Roy. Meteor. Soc., 137, 553–597, 2011. 5360

Dirmeyer, P. A., Xiang, G., Zhao, M., Zhichang, G., Oki, T., and Hanasaki, N.: GSWP-2: Multimodel analysis and implications for our perception of the land surface, B. Am. Meteorol. Soc., 87, 1381–1397, 2006. 5344

Domingues, T. F., Martinelli, L. A., and Ehleringer, J. R.: Ecophysiological traits of plant functional groups in forest and pasture ecosystems from eastern Amazonia, Brazil, Plant Ecol., 193, 101–112, 2007. 5375

Doughty, C. E. and Goulden, M. L.: Seasonal patterns of tropical forest leaf area index and CO_2 exchange, J. Geophys. Res.-Biogeo., 113, G00B06, doi:10.1029/2007JG000590, 2008. 5375

El Maayar, M., Price, D. T., Black, T. A., Humphreys, E. R., and Jork, E.-M.: Sensitivity tests of the integrated biosphere simulator to soil and vegetation characteristics in a Pacific coastal coniferous forest, Atmos. Ocean, 40, 313–332, 2002. 5344

Farquhar, G. D., Caemmerer, S., and Berry, J. A.: A biochemical model of photosynthetic CO_2 assimilation in leaves of C3 species, Planta, 149, 78–90, 1980. 5344

Friedlingstein, P., Cox, P., Betts, R., Bopp, L., Von Bloh, W., Brovkin, V., Cadule, P., Doney, S., Eby, M., Fung, I., Bala, G., John, J., Jones, C., Joos, F., Kato, T., Kawamiya, M., Knorr, W., Lindsay, K., Matthews, H. D., Raddatz, T., Rayner, P., Reick, C., Roeckner, E., Schnitzler, K.-G., Schnur, R., Strassmann, K., Weaver, A. J., Yoshikawa, C., and Zeng, N.: Climate–carbon cycle feedback analysis: results from the C4MIP model intercomparison, J. Climate, 19, 3337–3353, 2006. 5343

Galbraith, D., Levy, P. E., Sitch, S., Huntingford, C., Cox, P., Williams, M., and Meir, P.: Multiple mechanisms of Amazonian forest biomass losses in three dynamic global vegetation models under climate change, New Phytol., 187, 647–665, 2010. 5361

Gao, F., Morisette, J. T., Wolfe, R. E., Ederer, G., Pedelty, J., Masuoka, E., Myneni, R., Tan, B., and Nightingale, J.: An algorithm to produce temporally and spatially continuous MODIS-LAI time series, IEEE Geosci. Remote S., 5, 60–64, 2008. 5351

Gilmanov, T. G., Tieszen, L. L., Wylie, B. K., Flanagan, L. B., Frank, A. B., Haferkamp, M. R., Meyers, T. P., and Morgan, J. A.: Integration of CO_2 flux and remotely-sensed data for primary production and ecosystem respiration analyses in the Northern Great Plains: potential for quantitative spatial extrapolation, Global Ecol. Biogeogr., 14, 271–292, 2005. 5374

Gornall, J. L., Jónsdóttir, I. S., Woodin, S. J., and Van der Wal, R.: Arctic mosses govern below-ground environment and ecosystem processes, Oecologia, 153, 931–941, 2007. 5350

Goulden, M. L., Miller, S. D., Da Rocha, H. R., Menton, M. C., de Freitas, H. C., e Silva Figueira, A. M., and de Sousa, C. A. D.: Diel and seasonal patterns of tropical forest CO_2 exchange, Ecol. Appl., 14, 42–54, 2004. 5374

Grünwald, T. and Bernhofer, C.: A decade of carbon, water and energy flux measurements of an old spruce forest at the Anchor Station Tharandt, Tellus B, 59, 387–396, 2007. 5374, 5375

Hallgren, W. and Pitman, A.: The uncertainty in simulations by a Global Biome Model (BIOME3) to alternative parameter values, Glob. Change Biol., 6, 483–495, 2000. 5344

Haverd, V., Leuning, R., Griffith, D., van Gorsel, E., and Cuntz, M.: The turbulent Lagrangian time scale in forest canopies constrained by fluxes, concentrations and source distributions, Bound.-Lay. Meteorol., 130, 209–228, 2009. 5375

Henderson-Sellers, A., McGuffie, K., and Pitman, A. J.: The Project for Intercomparison of Land-Surface Parametrization Schemes (PILPS): 1992 to 1995, Clim. Dynam., 12, 849–859, 1996. 5344

Houldcroft, C. J., Grey, W. M. F., Barnsley, M., Taylor, C. M., Los, S. O., and North, P. R. J.: New vegetation albedo parameters and global fields of soil background albedo derived from MODIS for use in a climate model, J. Hydrometeorol., 10, 183–198, 2009. 5346

Hutyra, L. R., Munger, J. W., Saleska, S. R., Gottlieb, E., Daube, B. C., Dunn, A. L., Amaral, D. F., De Camargo, P. B., and Wofsy, S. C.: Seasonal controls on the exchange of carbon and water in an Amazonian rain forest, J. Geophys. Res.-Biogeo., 112, G03008, doi:10.1029/2006JG000365, 2007. 5374, 5375

Jones, C. P.: Unified Model Documentation Paper No 70: Ancillary File Data Sources, Tech. rep., UK Met Office, 2007. 5350

Kattge, J., Knorr, W., Raddatz, T., and Wirth, C.: Quantifying photosynthetic capacity and its relationship to leaf nitrogen content for global-scale terrestrial biosphere models, Glob. Change Biol., 15, 976–991, 2009. 5375

Kistler, R., Kalnay, E., Collins, W., Saha, S., White, G., Woollen, J., Chelliah, M., Ebisuzaki, W., Kanamitsu, M., Kousky, V., van den Dool, H., Jeanne, R., and Fiorino, M.: The NCEP-NCAR 50-year reanalysis: monthly means CD-ROM and documentation, B. Am. Meteorol. Soc., 82, 247–267, 2001. 5361

Knorr, W.: Annual and interannual CO_2 exchanges of the terrestrial biosphere: process-based simulations and uncertainties, Global Ecol. Biogeogr., 9, 225–252, 2000. 5344

Knorr, W. and Heimann, M.: Uncertainties in global terrestrial biosphere modeling: 1. A comprehensive sensitivity analysis with a new photosynthesis and energy balance scheme, Global Biogeochem. Cy., 15, 207–225, 2001. 5344

Laurila, T., Soegaard, H., Lloyd, C. R., Aurela, M., Tuovinen, J.-P., and Nordstroem, C.: Seasonal variations of net CO_2 exchange in European Arctic ecosystems, Theor. Appl. Climatol., 70, 183–201, 2001. 5374, 5375

Lawrence, P. J. and Chase, T. N.: Representing a new MODIS consistent land surface in the Community Land Model (CLM 3.0), J. Geophys. Res.-Biogeo., 112, G01023, doi:10.1029/2006JG000168, 2007. 5351

Le Quéré, C., Raupach, M. R., Canadell, J. G., Marland, G., Bopp, L., Ciais, P., Conway, T. J., Doney, S. C., Feely, R. A., Foster, P., Friedlingstein, P., Gurney, K., Houghton, R. A., House, J. I., Huntingford, C., Levy, P. E., Lomas, M. R., Majkut, J., Metzl, N., Ometto, J. P., Peters, G. P., Prentice, I. C., Randerson, J. T., Running, S. W., Sarmiento, J. L., Schuster, U., Sitch, S., Takahashi, T., Viovy, N., van der Werf, G. R., and Woodward, F. I.: Trends in the sources and sinks of carbon dioxide, Nat. Geosci., 2, 831–836, 2009. 5343

Leuning, R., Cleugh, H. A., Zegelin, S. J., and Hughes, D.: Carbon and water fluxes over a temperate Eucalyptus forest and a tropical wet/dry savanna in Australia: measurements and comparison with MODIS remote sensing estimates, Agr. Forest Meteorol., 129, 151–173, 2005. 5374

Liu, Q., Gu, L., Dickinson, R. E., Tian, Y., Zhou, L., and Post, W. M.: Assimilation of satellite reflectance data into a dynamical leaf model to infer seasonally varying leaf areas for climate and carbon models, J. Geophys. Res.-Atmos., 113, D19113, doi:10.1029/2007JD009645, 2008. 5357

Loveland, T. R., Reed, B. C., Brown, J. F., Ohlen, D. O., Zhu, Z., Yang, L., and Merchant, J. W.: Development of a global land cover characteristics database and IGBP DISCover from 1 km AVHRR data, Int. J. Remote Sens., 21, 1303–1330, 2000. 5350

Luo, Y. Q., Randerson, J. T., Abramowitz, G., Bacour, C., Blyth, E., Carvalhais, N., Ciais, P., Dalmonech, D., Fisher, J. B., Fisher, R., Friedlingstein, P., Hibbard, K., Hoffman, F., Huntzinger, D., Jones, C. D., Koven, C., Lawrence, D., Li, D. J., Mahecha, M., Niu, S. L., Norby, R., Piao, S. L., Qi, X., Peylin, P., Prentice, I. C., Riley, W., Reichstein, M., Schwalm, C., Wang, Y. P., Xia, J. Y., Zaehle, S., and Zhou, X. H.: A framework for benchmarking land models, Biogeosciences, 9, 3857–3874, doi:10.5194/bg-9-3857-2012, 2012. 5344

Meyers, T. P. and Hollinger, S. E.: An assessment of storage terms in the surface energy balance of maize and soybean, Agr. Forest Meteorol., 125, 105–115, 2004. 5374, 5375

Nachtergaele, F., van Velthuizen, H., Verelst, L., Wiberg, D., Batjes, N., Dijkshoorn, K., van Engelen, V., Fischer, G., Jones, A., Montanarella, L., Petri, M., Prieler, S., Teixeira, E., and Shi, X.: Harmonized World Soil Database v1.2, Tech. rep., International Institute for Applied Systems Analysis (IIASA), Food and Agriculture Organization of the United Nations (FAO), 2012. 5350

Pitman, A. J.: The evolution of, and revolution in, land surface schemes designed for climate models, Int. J. Climatol., 23, 479–510, 2003. 5343

Randerson, J. T., Hoffman, F. M., Thornton, P. E., Mahowald, N. M., Lindsay, K., Lee, Y.- H., Nevison, C. D., Doney, S. C., Bonan, G., Stöckli, R., Covey, C., Running, S. W., and Fung, I. Y.: Systematic assessment of terrestrial biogeochemistry in coupled climate–carbon models, Glob. Change Biol., 15, 2462–2484, 2009. 5344

Ryu, Y., Baldocchi, D. D., Ma, S., and Hehn, T.: Interannual variability of evapotranspiration and energy exchange over an annual grassland in California, J. Geophys. Res., 113, D09104, doi:10.1029/2007JD009263, 2008. 5374

Schaefer, K., Schwalm, C. R., Williams, C., Arain, M. A., Barr, A., Chen, J. M., Davis, K. J., Dimitrov, D., Hilton, T. W., Hollinger, D. Y., Humphreys, E., Poulter, B., Raczka, B. M., Richardson, A. D., Sahoo, A., Thornton, P., Vargas, R., Verbeeck, H., Anderson, R., Baker, I., Black, T. A., Bolstad, P., Chen, J., Curtis, P. S., Desai, A. R., Dietze, M., Dragoni, D., Gough, C., Grant, R. F., Gu, L., Jain, A., Kucharik, C., Law, B., Liu, S., Lokipitiya, E., Margolis, H. A., Matamala, R., McCaughey, J. H., Monson, R., Munger, J. W., Oechel, W., Peng, C., Price, D. T., Ricciuto, Dan Riley, W. J., Roulet, N., Tian, H., Tonitto, C., Torn, M., Weng, E., and Zhou, X.: A model–data comparison of gross primary productivity: results from the North American Carbon Program site synthesis, J. Geophys. Res.-Biogeo., 117, G03010, doi:10.1029/2012JG001960, 2012. 5344, 5346

Schimel, D.: Carbon cycle conundrums, P. Natl. Acad. Sci. USA, 104, 18353–18354, 2007. 5343

Schmid, H. P., Grimmond, C. S. B., Cropley, F., Offerle, B., and Su, H.-B.: Measurements of CO_2 and energy fluxes over a mixed hardwood forest in the mid-western United States, Agr. Forest Meteorol., 103, 357–374, 2000. 5374

Sellers, P. J., Dickinson, R. E., Randall, D. A., Betts, A. K., Hall, F. G., Berry, J. A., Collatz, G. J., Denning, A. S., Mooney, H. A., Nobre, C. A., Sato, N., Field, C. B., and Henderson-Sellers, A.: Modeling the exchanges of energy, water, and carbon between continents and the atmosphere, Science, 275, 502–509, doi:10.1126/science.275.5299.502, 1997. 5344

Sheffield, J., Goteti, G., and Wood, E. F.: Development of a 50-year high-resolution global dataset of meteorological forcings for land surface modeling, J. Climate, 19, 3088–3111, 2006. 5348, 5350, 5355

Stöckli, R., Lawrence, D. M., Niu, G. Y., Oleson, K. W., Thornton, P. E., Yang, Z. L., Bonan, G. B., Denning, A. S., and Running, S. W.: Use of FLUXNET in the Community Land Model development, J. Geophys. Res, 113, G01025, doi:10.1029/2007JG000562, 2008. 5344, 5374

GMDD
7, 5341–5380, 2014

Multi-site evaluation of the JULES land surface model using global and local data

D. Slevin et al.

Suni, T., Rinne, J., Reissell, A., Altimir, N., Keronen, P., Rannik, U., Kulmala, M., and Vesala, T.: Long-term measurements of surface fluxes above a Scots pine forest in Hyytiala, southern Finland, 1996–2001, Boreal Environ. Res., 8, 287–302, 2003. 5374, 5375

Urbanski, S., Barford, C., Wofsy, S., Kucharik, C., Pyle, E., Budney, J., McKain, K., Fitzjarrald, D., Czikowsky, M., and Munger, J. W.: Factors controlling CO_2 exchange on timescales from hourly to decadal at Harvard Forest, J. Geophys. Res, 112, G02020, doi:10.1029/2006JG000293, 2007. 5374

Weedon, G. P., Gomes, S., Viterbo, P., Shuttleworth, W. J., Blyth, E., Österle, H., Adam, J. C., Bellouin, N., Boucher, O., and Best, M.: Creation of the WATCH Forcing Data and its use to assess global and regional reference crop evaporation over land during the twentieth century, J. Hydrometeorol., 12, 823–848, 2011. 5348, 5349, 5355

Weedon, G. P., Gomes, S., Balsmao, G., Best, M., Bellouin, N., and Viterbo, P.: WFDEI announcement paper, 2012. 5348, 5349

Williams, M., Richardson, A. D., Reichstein, M., Stoy, P. C., Peylin, P., Verbeeck, H., Carvalhais, N., Jung, M., Hollinger, D. Y., Kattge, J., Leuning, R., Luo, Y., Tomelleri, E., Trudinger, C. M., and Wang, Y.-P.: Improving land surface models with FLUXNET data, Biogeosciences, 6, 1341–1359, doi:10.5194/bg-6-1341-2009, 2009. 5344

Yang, W., Tan, B., Huang, D., Rautiainen, M., Shabanov, N. V., Wang, Y., Privette, J. L., Huemmrich, K. F., Fensholt, R., Sandholt, I., Weiss, M., Ahl, D. E., Gower, S. T., Nemani, R. R., Knyazikhin, Y., and Myneni, R. B.: MODIS leaf area index products: from validation to algorithm improvement, IEEE T. Geosci. Remote, 44, 1885–1898, 2006. 5351

Table 1. Flux towers used in this study. The following biome types were used: Deciduous Broadleaf Forest (DBF), Evergreen Needleleaf Forest (ENF), Cropland (CRO), Grassland (GRA), Tundra (TUN), Evergreen Broadleaf Forest (EBF).

		Location					
Number	Site	Lat [°N]	Lon [°E]	Altitude (m)	Biome Type	Year	Climate Zone
1	Harvard Forest	42.54	−72.17	303	DBF	2008	Temperate
2	Tharandt	50.96	13.57	380	ENF	2003	Temperate
3	Bondville	40.01	−88.29	219	CRO	2000	Temperate
4	Fort Peck	48.31	−105.10	634	GRA	2004	Temperate
5	Morgan Monroe	39.32	−86.41	275	DBF	2007	Temperate
6	Tumbarumba	−35.66	148.15	1200	EBF	2008	Temperate
7	Kaamanen	69.14	27.29	155	TUN	2002	Boreal
8	Hyytiala	61.85	24.29	181	ENF	2003	Boreal
9	Santarem KM67	−2.86	−54.96	130	EBF	2003	Tropical
10	Santarem KM83	−3.02	−54.98	130	EBF	2001	Tropical
11	El Saler	39.35	−0.32	10	ENF	2003	Mediterranean
12	Vaira Ranch	38.41	−120.95	129	GRA	2005	Mediterranean

GMDD
7, 5341–5380, 2014

Multi-site evaluation of the JULES land surface model using global and local data

D. Slevin et al.

Table 2. Types of model simulations performed in this study.

	Model simulations	Parameter sets	Meteorological forcing	LAI[a]	Phenology[b]
Site-specific vs. global data	local-F	local	FLUXNET	Local	Default
	local-WEIG	local	WFDEI-GPCC	Local	Default
	global-WEIG	global	WFDEI-GPCC	Global	Default
	global-WEIC	global	WFDEI-CRU	Global	Default
	global-P	global	PRINCETON	Global	Default
Satellite phenology	local-FNM	local	FLUXNET	Site max. MODIS LAI	Default
	local-FM	local	FLUXNET	Site max. MODIS LAI	Daily forcing

[a] Local refers to the observed annual maximum LAI at each site and global refers to that obtained from the look-up tables used by the global operational version of the model.
[b] Default refers to the default phenology model used by JULES and daily forcing means that the default phenology has been switched off and the model forced with daily MODIS LAI.

GMDD
7, 5341–5380, 2014

Table 3. Vegetation (PFT) and non-vegetation land cover type (BL: broadleaf tree, NL: needle-leaf tree, C3g: C3 grass, C4g: C4 grass, sh: shrubs, bs: bare soil) fractions at the 12 FLUXNET sites. For each site, the first row refers to global data and the second refers to site-specific (local).

			Plant Functional Types						
Site	IGBP value	IGBP class	BL	NL	C3g	C4g	sh	bs	References
Harvard Forest	4	DB forest	0.60		0.05	0.10	0.05	0.20	
		DB forest	0.95					0.05	Urbanski et al. (2007)
Vaira Ranch	8	Woody savannah	0.50		0.15		0.25	0.10	
		Grassland			0.95			0.05	Ryu et al. (2008)
Morgan Monroe	4	DB forest	0.60		0.05	0.10	0.05	0.20	
		DB forest	0.90					0.10	Schmid et al. (2000)
Hyytiala	1	EN forest		0.70	0.20			0.10	
		EN forest		0.95				0.05	Suni et al. (2003)
Tharandt	5	Mixed forest	0.35	0.35	0.20			0.10	
		EN forest		0.95				0.05	Grünwald and Bernhofer (2007)
Tumbarumba	2	EB forest	0.85			0.10		0.05	
		EN forest		0.90				0.10	Leuning et al. (2005)
El Saler	7	Open shrub			0.05	0.10	0.35	0.50	
		EN forest		0.90				0.10	Stöckli et al. (2008)
Fort Peck	10	Grassland			0.70	0.15	0.05	0.10	
		Grassland			0.90			0.10	Gilmanov et al. (2005)
Kaamanen	1	EN forest		0.70	0.20			0.10	
		Grassland			0.90			0.10	Laurila et al. (2001)
Santarem KM67	2	EB forest	0.85			0.10		0.05	
		EB forest	0.98					0.02	Hutyra et al. (2007)
Santarem KM83	2	EB forest	0.85			0.10		0.05	
		EB forest	0.98					0.02	Goulden et al. (2004)
Bondville	12	Cropland			0.75	0.05		0.20	
		Grassland			0.90			0.10	Meyers and Hollinger (2004)

GMDD
7, 5341–5380, 2014

Multi-site evaluation of the JULES land surface model using global and local data

D. Slevin et al.

Table 4. Site-specific and global biophysical parameters (site annual maximum LAI, canopy height and V_{cmax}) and $\sum GPP_{obs}$ (FLUXNET Is observed annual sum) at the 12 FLUXNET sites. For each site, the first row refers to global data, the second refers to local and the third refers to satellite. Online data was accessed in April 2013.

Site	LAI ($m^2\,m^{-2}$)	Canopy height (m)	V_{cmax} ($\mu mol\,CO_2\,m^{-2}\,s^{-1}$)	$\sum GPP_{obs}$ ($gC\,m^{-2}\,year^{-1}$)	References
Harvard Forest	5.00 5.00[a] 6.03	19.01 24.00[a] –	32.00 35.20[a] –	1621	[a]Harvard Forest Data Archive/Exchange
Vaira Ranch	4.00 2.74[b] 3.46	1.26 0.67[b] –	48.00 42.25[c] –	1047	[b] Ameriflux Biological Data [c] Beerling and Quick (1995)
Morgan Monroe	5.00 5.23[b] 6.81	19.01 27.00[b] –	32.00 34.80[c] –	1385	
Hyytiala	6.00 3.00[d] 4.56	21.46 14.00[e] –	24.00 60.00[d] –	997	[d] P. Kolari, personal communication, 2013 [e] Suni et al. (2003)
Tharandt	6.00 7.10[f] 3.82	21.46 26.50[g] –	24.00 62.50[h] –	1754	[f] T. Grünwald, personal communication, 2013 [g] Grünwald and Bernhofer (2007) [h] Kattge et al. (2009)
Tumbarumba	4.00 2.50[i] 6.08	16.38 40.00[j] –	24.00 74.33[k] –	2806	[i] E. van Gorsel, personal communication, 2013 [j] Cleugh et al. (2007) [k] Haverd et al. (2009)
El Saler	4.00 4.00[l] 1.04	16.38 12.00[m] –	24.00 62.5[h] –	1512	[l] Blyth et al. (2010) [m] Obtained from http://www.bgc-jena.mpg.de
Fort Peck	3.00 2.00[l] 1.41	1.04 0.40[n] –	48.00 42.25[s] –	367	[n] Obtained from http://ameriflux.ornl.gov/
Kaamanen	2.00 0.70[o] 1.33	0.79 1.00[p] –	48.00 42.25[c] –	368	[o] Laurila et al. (2001) [p] Aurela et al. (1998)
Santarem Km67	9.00 5.25[q] 6.73	28.12 45.00[r] –	32.00 81.00[s] –	3171	[q] Oak Ridge National Laboratory DAAC [r] Hutyra et al. (2007) [s] Domingues et al. (2007)
Santarem Km83	9.00 6.00[t] 6.63	28.12 40.00[u] –	32.00 81.00[v] –	2724	[t] Doughty and Goulden (2008) [u] Bruno et al. (2006) [v] Domingues et al. (2007)
Bondville	5.00 6.74[b] 3.37	1.46 0.90[w] –	48.00 117.35[c] –	766	[w] Meyers and Hollinger (2004)

GMDD
7, 5341–5380, 2014

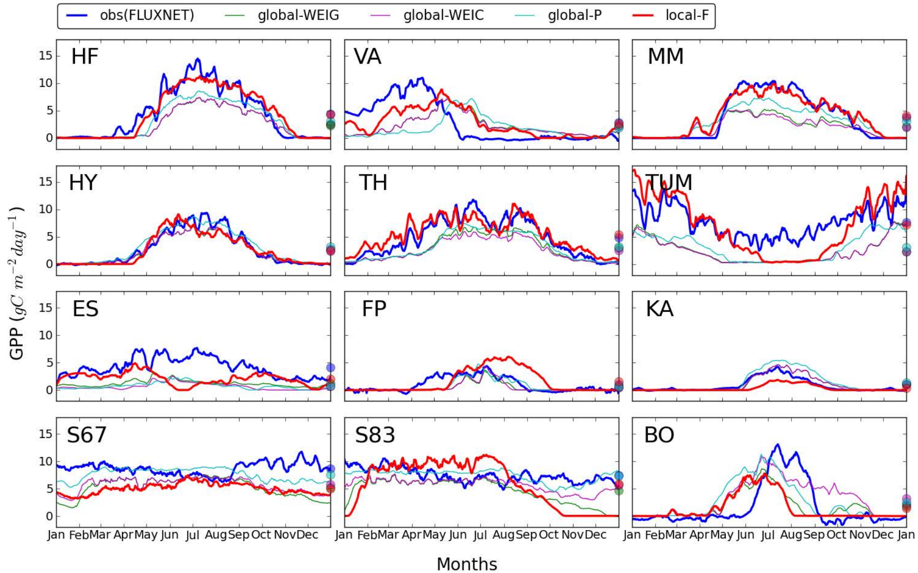

Figure 1. Seasonal cycle of model-predicted (local-F, global-WEIG, global-WEIC and global-P in Table 2) and observed GPP fluxes, smoothed with a 7 day moving average window, at the 12 FLUXNET sites (HF: Harvard Forest, VA: Vaira Ranch, MM: Morgan Monroe, HY: Hyytiala, TH: Tharandt, TUM: Tumbarumba, ES: El Saler, FP: Fort Peck, KA: Kaamanen, S67: Santarem Km67, S83: Santarem Km83, BO: Bondville). Model simulation years are given in Table 1. The thick lines refer to FLUXNET observations (blue) and simulated GPP from local-F model simulations (red). Annual averages for model simulations and observations are plotted as thick dots on right of each plot in the same colours.

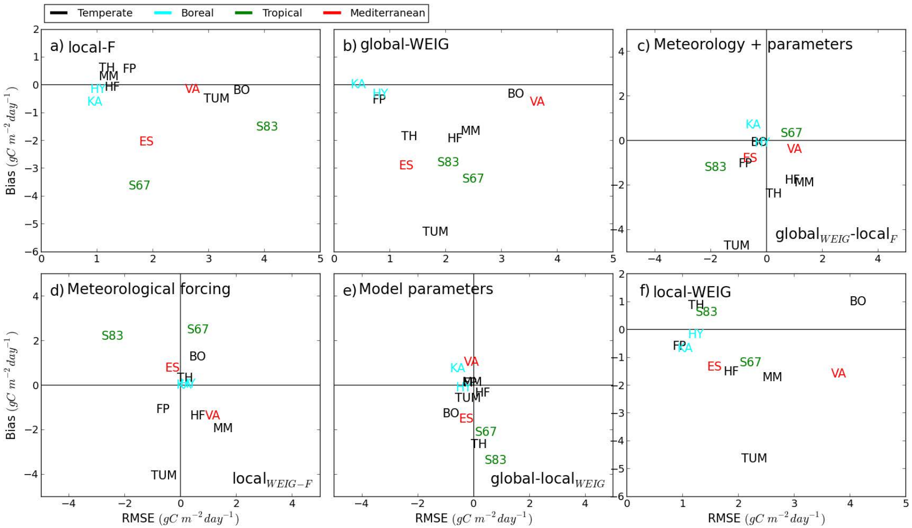

Figure 2. Comparison of modelled and observed GPP using bias and RMSE at the 12 FLUXNET sites (HF: Harvard Forest, VA: Vaira Ranch, MM: Morgan Monroe, HY: Hyytiala, TH: Tharandt, TUM: Tumbarumba, ES: El Saler, FP: Fort Peck, KA: Kaamanen, S67: Santarem Km67, S83: Santarem Km83, BO: Bondville) for three sets of model simulations; **(a)** local-F, **(b)** global-WEIG and **(f)** local-WEIG (Table 2). **(c)** displays the differences between bias and RMSE for global-WEIG and local-F model simulations, **(d)** differences between local-WEIG and local-F model simulations and **(e)** differences between global-WEIG and local-WEIG model simulations. Marked on **(c)**, **(d)** and **(e)** next to the figure letter are how the sets of model simulations differ. The site labels are coloured according to their climate zone (Table 1).

GMDD
7, 5341–5380, 2014

Title Page
Abstract Introduction
Conclusions References
Tables Figures
◄ ►
◄ ►
Back Close
Full Screen / Esc
Printer-friendly Version
Interactive Discussion

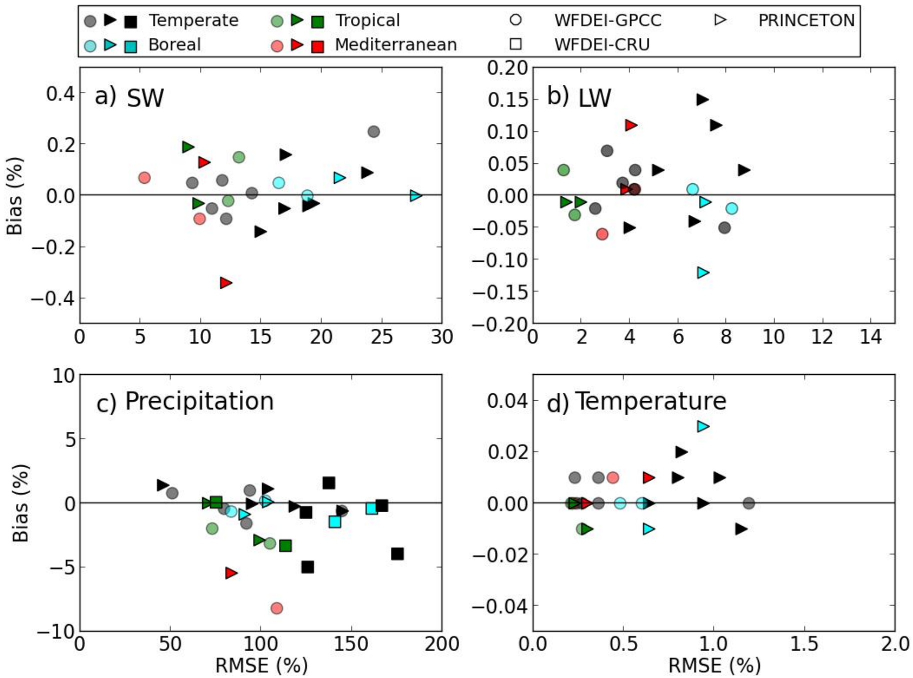

Figure 3. Bias and RMSE, expressed as percentages of daily average, when comparing global (WFDEI-GPCC (circles), WFDEI-CRU (squares) and PRINCETON (triangles)) to local meteorological data for four meteorological variables; **(a)** downward shortwave radiation (SW), **(b)** downward longwave radiation (LW), **(c)** precipitation and **(d)** surface air temperature, at the 12 FLUXNET sites (HF: Harvard Forest, VA: Vaira Ranch, MM: Morgan Monroe, HY: Hyytiala, TH: Tharandt, TUM: Tumbarumba, ES: El Saler, FP: Fort Peck, KA: Kaamanen, S67: Santarem Km67, S83: Santarem Km83, BO: Bondville). The site labels are coloured according to their climate zone (Table 1). Note that before computing bias and RMSE, the meteorological data was converted to dimensionless quantities by dividing the daily time series by the yearly mean.

GMDD
7, 5341–5380, 2014

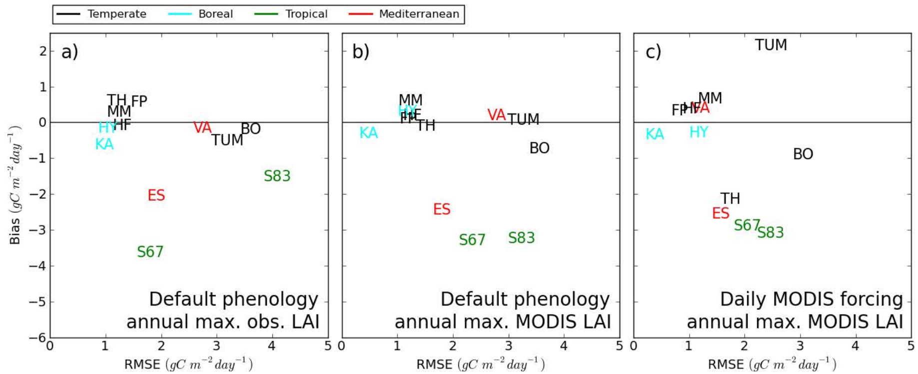

Figure 4. Comparison of modelled and observed GPP using bias and RMSE (computed using anomalies) at the 12 FLUXNET sites (HF: Harvard Forest, VA: Vaira Ranch, MM: Morgan Monroe, HY: Hyytiala, TH: Tharandt, TUM: Tumbarumba, ES: El Saler, FP: Fort Peck, KA: Kaamanen, S67: Santarem Km67, S83: Santarem Km83, BO: Bondville) for three sets of model simulations; **(a)** default phenology model with locally observed annual maximum LAI (data values used same as in Fig. 2a (local-F)), **(b)** default phenology model with annual maximum MODIS LAI (model simulations local-FNM) and **(c)** daily MODIS forced model simulations with annual maximum MODIS LAI (model simulations local-FM). The site labels are coloured according to their climate zone (Table 1).

GMDD
7, 5341–5380, 2014

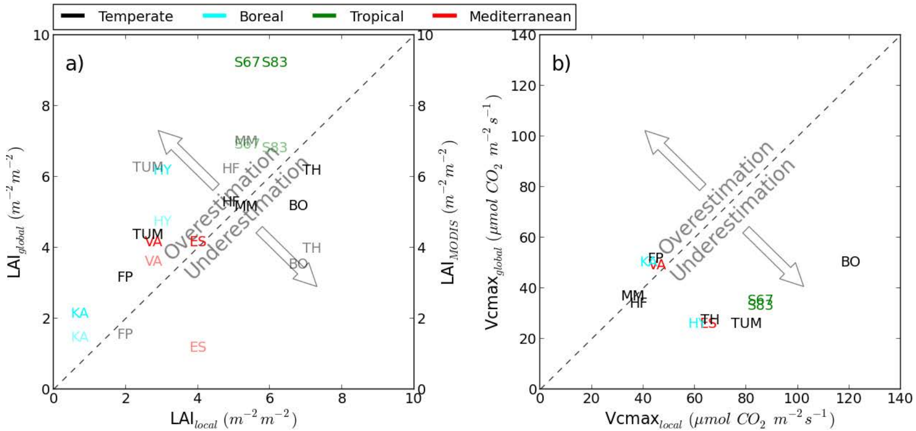

Figure 5. Comparison of global, MODIS (site annual maximum) and local Leaf Area Index (LAI) and maximum rate of Rubisco carboxylase activity (V_{cmax}) at the 12 FLUXNET sites (HF: Harvard Forest, VA: Vaira Ranch, MM: Morgan Monroe, HY: Hyytiala, TH: Tharandt, TUM: Tumbarumba, ES: El Saler, FP: Fort Peck, KA: Kaamanen, S67: Santarem Km67, S83: Santarem Km83, BO: Bondville). The LAI data displayed for each study site refer to the annual maximum LAI of the dominant PFT. The site labels are coloured according to their climate zone (Table 1). The dashed grey lines represent LAI and V_{cmax}, where global, MODIS and local values match, with overestimated global and MODIS values above the dashed line and underestimated values below it.